Detecting microbial engraftment after FMT: sorting signals from noise using placebo sequencing and culture-enriched metagenomics

Shahrokh Shekarriz[1,2], Jake C. Szamosi[1,2], Fiona J. Whelan[3], Jennifer T. Lau[2], Josie Libertucci[2], Laura Rossi[2,4], Michelle E. Fontes[1,2], Melanie Wolfe[2], Christine H. Lee[5], Paul Moayyedi[1,2], and Michael G. Surette[1,2,4]

[1]Department of Medicine, McMaster University
[2]Farncombe Family Digestive Health Research Institute McMaster University
[3]School of Biological Sciences, University of Manchester
[4]Department of Biochemistry and Biomedical Sciences, McMaster University
[5]Department of Pathology and Laboratory Medicine, The University of British Columbia

ABSTRACT

Fecal microbiota transplantation (FMT) has shown efficacy for the treatment of ulcerative colitis but with variable response between patients and trials. The mechanisms underlying FMT's therapeutic effects remains poorly understood but is generally assumed to involve engraftment of donor microbiota into the recipient's microbiome. Previous studies have reported microbial engraftment following FMT in various disease contexts but with inconsistent results between studies. Here we investigate engraftment in UC patients receiving FMT from a single donor applying amplicon-based profiling, shotgun metagenomics and culture-enriched metagenomics. Placebo samples were included to estimate engraftment noise, and a significant level of false-positive engraftment was observed which confounds the prediction of true engraftment. We show that analyzing engraftment across multiple patients from a single donor enhances the accuracy of detection. We identified a unique set of genes engrafted in responders to FMT which supports strain displacement as the primary mechanism of engraftment in our cohort.

32 Ulcerative colitis (UC) is a type of inflammatory bowel disease (IBD) of unknown etiology that is
33 restricted to the colon[1]. UC is believed to arise from a disruption in the balance between the
34 immune system and microbiota in a genetically susceptible individual[2]. Current standard medical
35 treatments have focused on supressing the immune response and are not always effective at
36 controlling disease[4]. An alternative approach is to alter the microbial environment responsible
37 for driving the immune response[5]. Fecal microbiota transplantation (FMT) has emerged as an
38 increasingly popular approach to alter the colonic microbiota[6] and is a standard therapy for
39 patients with recurrent *Clostridioides difficile* infection (rCDI)[7,8] and has also been evaluated in
40 UC[9–12].
41
42 We reported the first randomized controlled trial (RCT) of FMT for patients with active UC[5]. This
43 RCT showed that the proportion of patients with active UC in which remission was induced after
44 FMT (24%) was significantly higher than a placebo group (5%), with no difference in adverse
45 events. This has been replicated by other researchers and a systematic review of 12 RCTs suggests
46 there is moderate quality evidence that FMT can induce remission in active UC[13]. One of the
47 donors involved in our trial was more successful at inducing remission than other donors, with 7
48 of the 9 responders receiving Donor B stool[5]. This apparent donor effect can only be studied in
49 trials where each patient receives all their FMT from a single donor and most studies do not give
50 FMT in this way. Our RCT did use single donors for each participant with only a small pool of
51 donors overall[5]. We were therefore positioned to study donor effects, and we are building on
52 our previous work by further investigating the microbial composition of patients who received
53 FMT from Donor B compared to those who received placebo treatments to ask whether a specific
54 group of microbes were engrafted following FMT, and to determine whether microbial
55 engraftment is associated with remission after FMT.
56
57 Previous studies have reported microbial engraftment—the transfer of microbes from donor to
58 patients—following FMT in various disease contexts, particularly in rCDI[14–18]. However, there are
59 inconsistent results between studies. Even larger studies, which applied their bioinformatic
60 workflows to multiple publicly available datasets and disease types[19–21], reported disparate
61 outcomes. To our knowledge, none of these studies have applied their analytical pipelines to

placebo samples from RCTs sequenced with a metagenomic approach to assess background noise or establish thresholds for engraftment detection. Moreover, culture-independent approaches often lack the sensitivity to detect low-abundance bacteria. Culture-enriched sequencing methods provide a more comprehensive view of the human microbiome than culture-independent sequencing, particularly for low-abundance bacteria, and past studies have shown the utility of this approach in capturing the diversity of intestinal[22,23], lung[24,25], skin[26], and urine[27] human microbiota.

To answer the question of whether specific groups of microbes are responsible for inducing remission in UC, we have therefore used three high-throughput sequencing approaches; culture-independent (direct) 16S rRNA gene amplicon sequencing, culture-independent (direct) shotgun metagenomic sequencing (DMG), and culture-enriched shotgun metagenomic sequencing (CEMG). Further, we asked whether observed engraftment truly reflected the donor microbiome's influence, or if it was an artefact of low sampling resolution. To address this, we used a unique dataset, containing stool samples from patients receiving FMT from a single donor and those procured from patients undergoing placebo treatments. This multifaceted approach enables us to provide insights into the microbiome's potential role in UC remission.

Results

Our RCT involved 70 patients, with 36 undergoing FMT and 34 receiving a placebo[5]. At the trial's conclusion, 9 patients in the FMT group (7 from Donor B) and 2 in the placebo group had entered remission **(Figure 1A)**. For an accurate assessment of true microbial engraftment from Donor B, we revisited the 16S rRNA gene amplicon sequencing data with enhanced resolution by using amplicon sequence variants (ASV)[28] instead of operational taxonomic units (OTUs). This reanalysis involved paired pre- and post-treatment samples from 20 FMT recipients of Donor B's stool, and 31 placebo recipients **(Figure 1B).** We selected all available responders and an equal number non-responders from the Donor B FMT group (6 per group) and both responders and 10 non-responders (chosen at random) from the placebo groups for shotgun metagenomics. Additionally, shotgun metagenomic sequencing was applied to four longitudinal samples from

91 Donor B **(Figure 1C)**. We built a comprehensive sequence library of Donor B's samples via culture-
92 enriched metagenomic sequencing, assembly, and annotations previously described[25] **(Figure**
93 **1D,** see Supplementary Results**, Supp Figure 2).**
94

95 ## Microbial engraftment is present after FMT against a background of false positives.
96

97 We have previously shown that culture-independent methods often underestimate microbial
98 diversity in a stool sample compared to culture-enriched approaches[22]. If strains shared between
99 patient and donor below the detection limit of the culture-independent method in the patient
100 but are detected post-FMT they would appear as engrafted but are false-positives (spurious
101 engraftment). Here we compare measurements of engraftment in FMT recipients from a single
102 donor and placebo recipients to estimate the extent of spurious engraftment at different
103 sequencing resolutions, including at the ASV, species (as identified by MetaPhlAn4[29]), and strain
104 levels (as identified by StrainPhlAn4[29]).

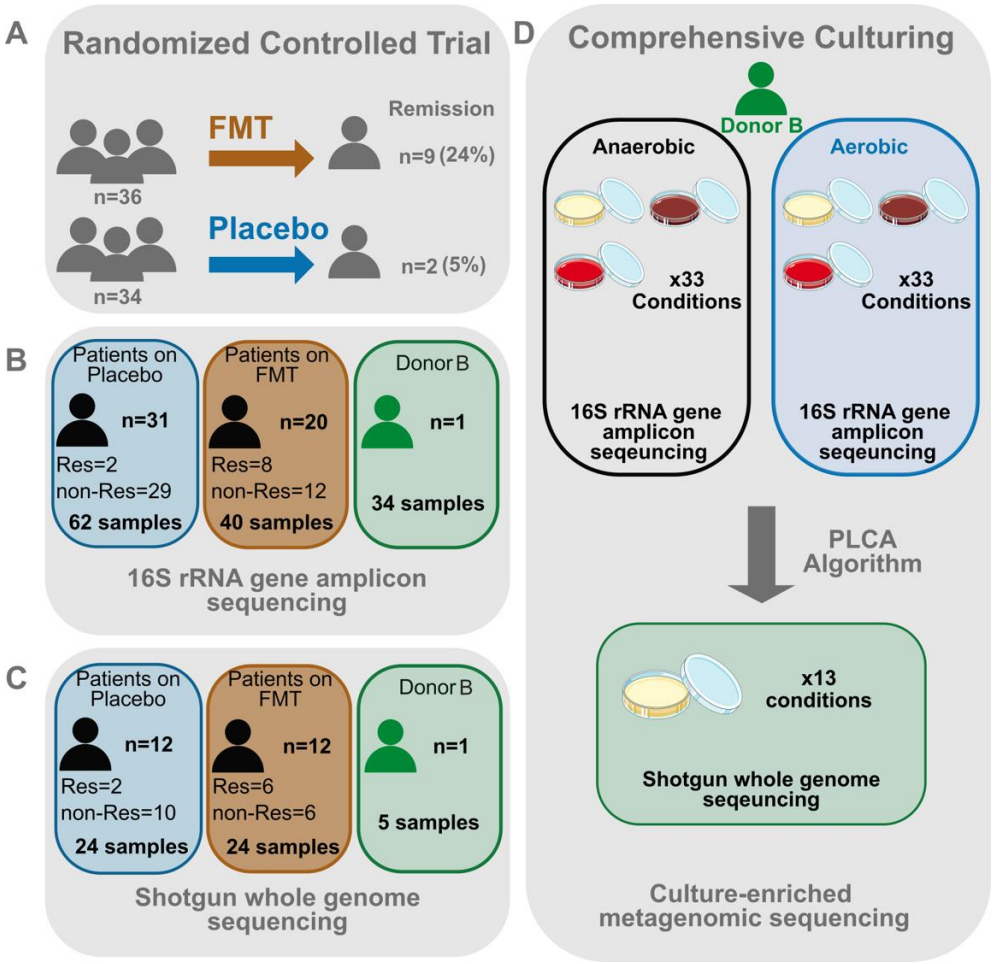

Figure 1. **Diagram of study design**. **A.** The double-blind randomized control trial of FMT for UC patients [5]. **B.** Direct 16S rRNA gene amplicon sequencing of stool was conducted for all patients and Donor B samples. Note that no baseline sample was available for one of the Donor B responders and this subject was excluded from our analysis. **C** Shotgun metagenomic sequencing was carried out for a subset of patients who received FMT from Donor B. 6 responders and 6 non-responders and an equivalent number of placebo treated patients. **D.** The culture-enriched metagenomics workflow to build a comprehensive sequence database of Donor B's gut microbiome. FMT = fecal microbiome transplant; PLCA = plate coverage algorithm.

We hypothesized that spurious engraftment in the placebo group would be minimal, and that significant microbial engraftment would correlate with clinical remission after FMT. To investigate this, we utilized samples from Donor B in both 16S rRNA and shotgun metagenomics sequencing datasets, establishing a stringent cut-off to define apparent microbial engraftment. A microbe was only described as engrafted if its relative abundance was zero prior to FMT and rose above our established cut-off after FMT (detailed in Methods, **Supp Figure 1**).

121 Initially, we investigated whether a clear difference exists between rates of apparent
122 engraftment in the FMT and placebo groups. Our dataset, involving a single donor, allowed us to
123 identify features that were apparently engrafted in multiple patients. We hypothesize that
124 engraftments observed in multiple individuals are more likely to be the result of true microbial
125 colonization and less reflective of individual-specific microbial changes during FMT. We identified
126 ASVs, species, and strains that appeared to be engrafted in a given numbers of patients ranging
127 from one, two, three, etc. from both FMT and placebo groups **(Figure 2 A1, B1, and C1)**. We then
128 computed the differences in numbers of each type of engraftment event for each dataset (donor
129 vs placebo) and used permutation tests to determine whether the amount of apparent
130 engraftment observed in patients who received FMT was significantly different from the amount
131 observed in placebo (see Methods). The results showed that the FMT group had a significantly
132 higher number of apparent engraftments than the placebo group (p-values presented in **Figure**
133 **2** for each dataset), highlighting the likelihood that FMT leads to (at least some) true engraftment.
134 However, a high number of spurious engraftments were also observed in the placebo group at
135 ASV, species, and strain levels, even with our stringent cut-off, suggesting considerable noise in
136 microbial engraftment detection.
137
138 Next, we identified apparently engrafted ASVs, species, and strains that were unique to either
139 the FMT or placebo groups, or shared between them ("overlap"), as shown in **Figure 2 A2**, **B2**,
140 and **C2**. The shotgun metagenomic dataset contained a stronger signal than the 16S dataset,
141 showing that a higher proportion of apparently engrafted features are unique to the FMT group.
142 More interestingly, the number of apparent engraftments in three or more patients in the
143 unique-to-placebo group – which was smaller than in the unique-to-FMT group across species,
144 strain, and 16S data - showed a stronger signal in species- and strain-level analysis. This indicates
145 that our approach of looking for features that appear to engraft in multiple patients reduces the
146 risk of spurious detection of engraftment. The number of apparently engrafted features that
147 were observed in both FMT and placebo groups underscores the importance of including placebo
148 sequencing in studies, and reflects the fact that common microbial changes in individuals over
149 time can mimic an engraftment signal.

Last, we explored whether microbial engraftment is associated with the response to FMT treatment. We compared the number of apparently engrafted features in responder and non-responder patients in the FMT group across ASV, species, and strain-level datasets **(Figure 2 A3, B3, C3)**. The 16S dataset included 14 non-responders and 6 responders, while the shotgun metagenomic datasets included the same 6 responders and a sub-set of non-responders (n=6). Similar to the placebo vs. FMT comparisons described above, we calculated the differences in the number of engrafted features and weighted engraftment statistics (see Methods) and used permutation tests to compare the two groups. The results indicated no clear difference in the number of apparent engraftments between responders and non-responders. Numbers of apparently engrafted features can be found in **Supplementary Table 2** and **3**.

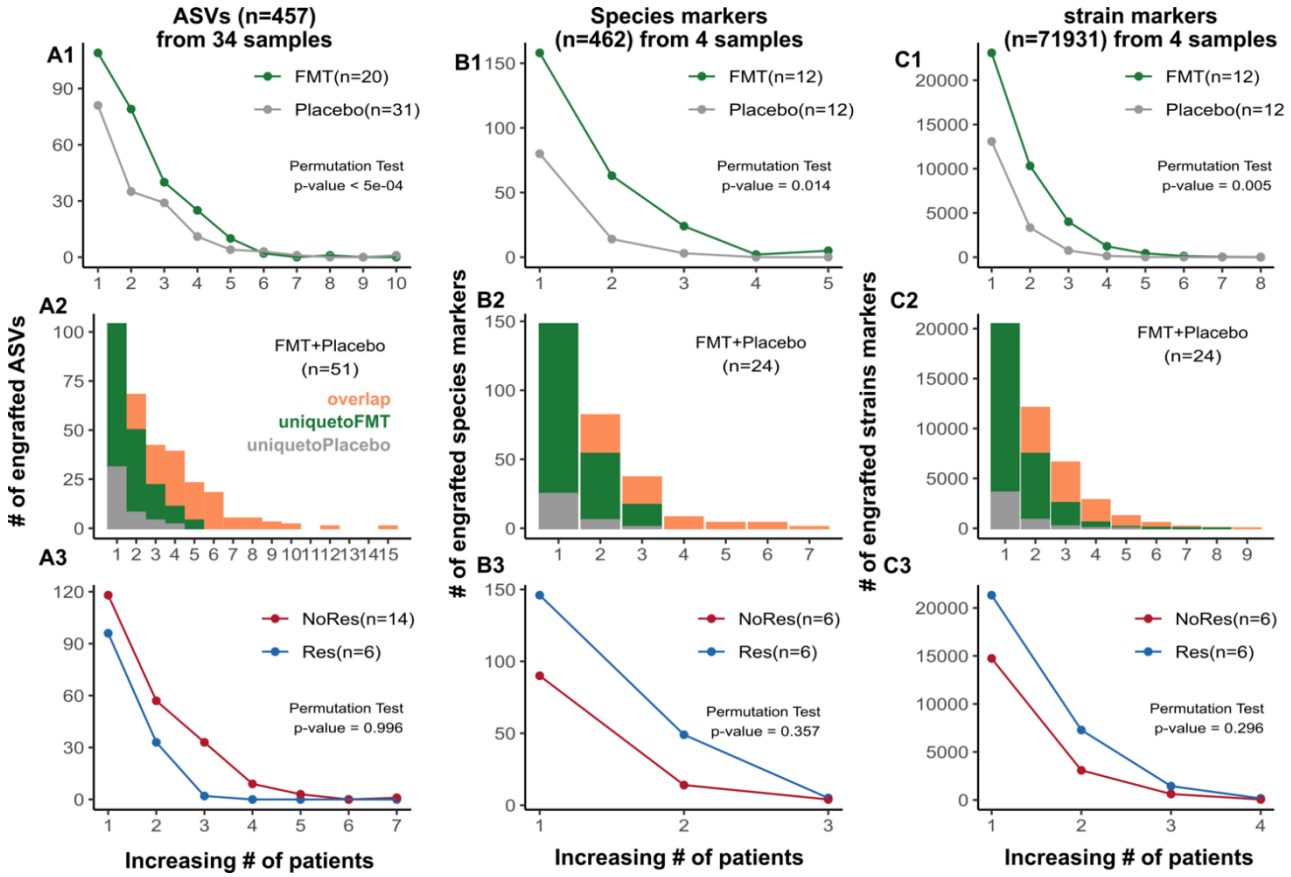

Figure 2. **Comparison of rates of apparent engraftment between groups**. Detection of apparently engrafted ASVs from 16S rRNA gene sequencing (A), species from shotgun metagenomic sequencing (B) and strains from shotgun metagenomic sequencing (C). Row 1: Comparison of the number of apparently engrafted features observed in FMT vs. placebo samples. The x-axis shows the number of patients a feature is apparently engrafted present in, and the y-axis shows the number of features observed to be apparently engrafted in exactly that many patients within FMT (green) or placebo (grey) samples. Row 2: Counting the number of apparently engrafted features that are unique to FMT samples (green), placebo samples (grey), or present in both (orange). The x-axis shows the number of patients a feature is apparently engrafted in, and the y-axis shows the number of features observed apparently engrafted in exactly that many patients. Row 3: The number of apparently engrafted features in FMT samples that are present in patients who responded to FMT treatment (blue lines) and did not respond (red lines). The differences between the points on the green and grey (row 1) or blue and red (row 3) lines were used to calculate the test statistics for the permutation tests.

High resolution mapping of patient reads to Donor B MAGs to detect apparent genome engraftment.

The results above indicate that detection of microbial engraftment may require greater microbial resolution than amplicon-based or read-based shotgun metagenomic sequencing. We hypothesized that co-assembling sequences from direct and culture-enriched metagenomic sequencing (CEMG) of the Donor B microbiota would improve gene and metagenome assembled genome (MAG) recovery from this donor compared to the commonly used direct metagenomic (DMG) approach. To generate the highest possible resolution assembly of Donor B's microbiota, we built a comprehensive database using a co-assembly of four longitudinal DMG samples as well as our single CEMG sample (see Supplementary Results, **Supp Figure 2**). We focused on 209 MAGs out of a total of 447 bins in our databases**.** To track the engraftment of these MAGs after FMT, we mapped raw shotgun reads — subsampled to uniform sequencing depth — from the pre- and post-treatment samples of 24 patients (12 FMT recipients and 12 placebo-treated individuals, 48 samples in total) to these 209 MAGs.

To define the thresholds for MAG engraftment, we mapped raw sequence reads from our four Donor B samples to the Donor B MAG database (BDB). In each sample, we observed bimodal distribution in MAG coverage, with the modes at the extremities of the distribution. We reasoned that MAGs that were present in that sample were the ones that appeared in the upper mode, where at least 75% of the length of the MAG was covered at least 1x, and the MAGS that were absent from that sample were those that appeared in the lower mode, where no more than 20%

200 of the length of the MAG was covered at least 1x. We therefore set these coverage values as our
201 cutoffs for presence and absence, respectively (**Supp Figure 1**).
202
203 We assessed the number of apparently engrafted MAGs in FMT recipients compared to placebo
204 recipients, using methods similar to those in the read-based metagenomic analyses described
205 above. Our goal was to determine if assembly-based assessments would reveal clear differences
206 between the FMT and placebo groups. Consistent with previous results, we found a significant
207 increase in the number of MAGs apparently engrafted in any given number of patients in the FMT
208 group compared to placebo (**Figure 3A1**, permutation test p=0.008). We observed no significant
209 differences in the numbers of engrafted MAGS, or the numbers of patients per engrafted MAG,
210 when comparing FMT responders to non-responders (**Figure 3A3**, permutation test p=0.24).
211
212 Upon examining MAGs engrafted in one or more individuals, we found that 57% of engrafted
213 MAGs (42 out of 74) were unique to patients who received and responded to FMT (**Figure 3B**),
214 specifically patients 4, 10, and 56. *Lachnospiraceae*, *Ruminococcaceae*, and *Oscillospiraceae* were
215 the most abundant families among these MAGs (**Figure 3C**). These findings suggest that microbial
216 genomic alterations in response to FMT are individual-specific, and that a degree of spurious
217 engraftment is observable in the placebo group, indicating that even genome-resolved
218 metagenomic approaches to detect engraftment are also prone to false positives.
219
220
221

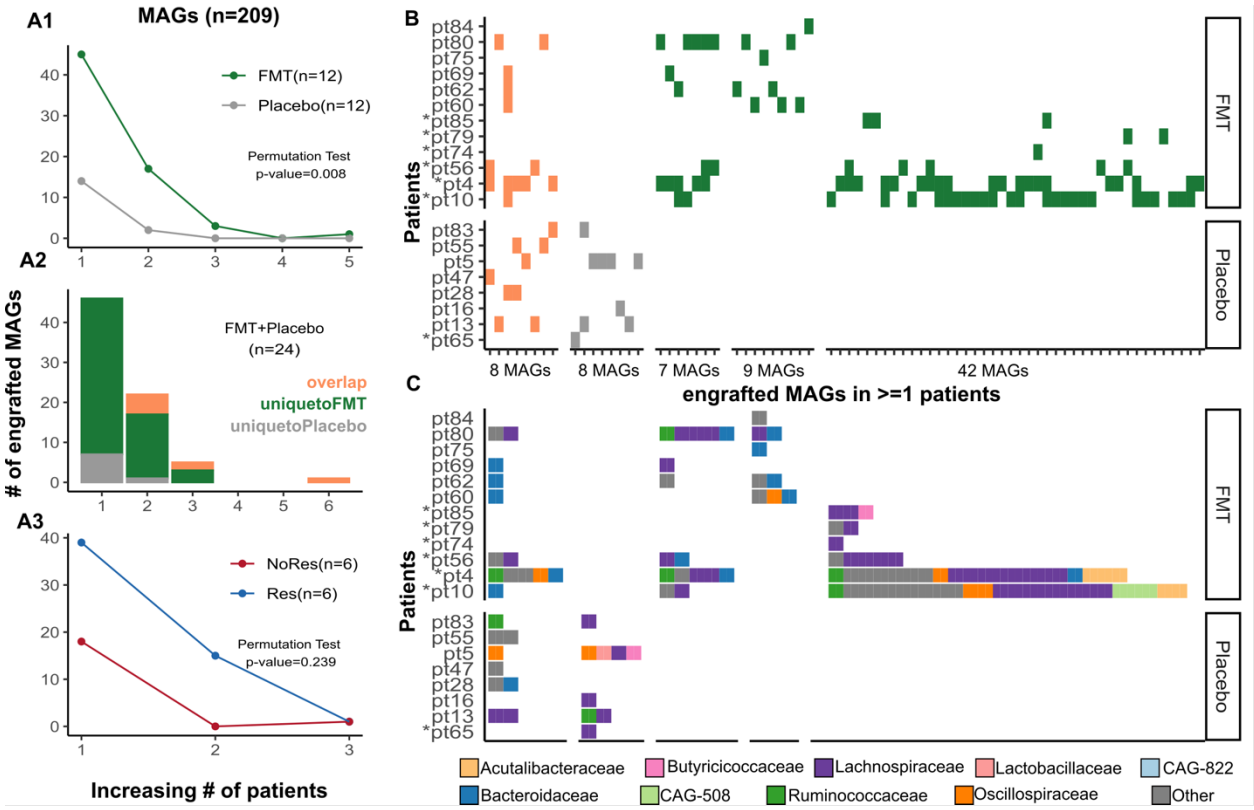

Figure 3. **High resolution genome-resolved metagenomics reveals apparent microbial genome engraftment following FMT**. **A1.** Comparison of apparently engrafted MAGs in patients who received FMT (n=12) vs. placebo (n=12) treatment. The x-axis displays number of patients in which a given MAG appears engrafted. **A2.** Counts of MAGs engrafted in only FMT (green), only Placebo (grey), and both (orange). **A3.** MAGs engrafted in FMT patients, observed in responders (n=6, blue) and non-responders (n=6, red). The differences between the points on the green and grey (A1) or blue and red (A3) lines were used to calculate the test statistics for the permutation tests. **B.** All donor MAGs engrafted in at least one patient. Green represents MAGs exclusively engrafted in FMT recipients, grey indicates MAGs spuriously detected as engrafted in the Placebo group, and orange signifies MAGs detected in both FMT and Placebo treatment cohorts. MAGs are ordered on the x axis by which group(s) of patients they were apparently engrafted in. **C.** The family-taxonomy of donor MAGs engrafted in at least one patient.

A signature of gene engraftment in patients who responded to FMT.

Although our approach allowed us to refine 209 MAGs from a single FMT donor, tracking MAGs omits information from the majority of assembled reads, which are in bins or contigs that are excluded from MAGs. In strains or species that are closely related, for instance, the presence or absence of a few genes can lead to distinct functional profiles[30,31]. Therefore, detecting strain replacement events following FMT requires analysis of bacterial genes. Furthermore, MAGs do not usually represent complete genomes[32]. This complexity is further evidenced by the Donor B MAGs, where we found that 20% of donor MAGs had 1x read coverage in post-FMT samples over

243 20-75% of their genome , and could therefore not be determined to be definitively present or
244 absent in any patient samples **(Supp Figure 1)**
245
246 We aimed to identify genes linked with engraftment and response to FMT. Using all Donor B
247 contigs >2.5kb long, we identified a total of 755,662 genes. We then mapped raw reads from all
248 the patient samples (n=48), to the Donor B gene database. We define apparently engrafted genes
249 as those with ≤ 1x coverage over less than 25% of their length in the baseline sample, and ≥ 1x
250 coverage over 90% or more of their length after treatment.
251
252 We employed the same methodology used in 16S, read-based metagenomics, and MAG analysis
253 to assess engraftment in the FMT and placebo groups, to again identify the rate of spurious
254 engraftment. Our results revealed a significant difference in the number of apparently engrafted
255 genes between patients treated with FMT and those receiving placebo (**Figure 4A1**, permutation
256 test p=0.001). Consistent with all previous analyses, the number of apparently engrafted genes
257 unique to the placebo group decreased as we restricted the count to genes apparently engrafted
258 in increasing numbers of patients (**Figure 4A2**). Consistent with other datasets, we could not
259 clearly see a difference in the number of engrafted genes between responders and non-
260 responders within the FMT group (**Figure 4A3,** permutation test p=0.86).
261
262

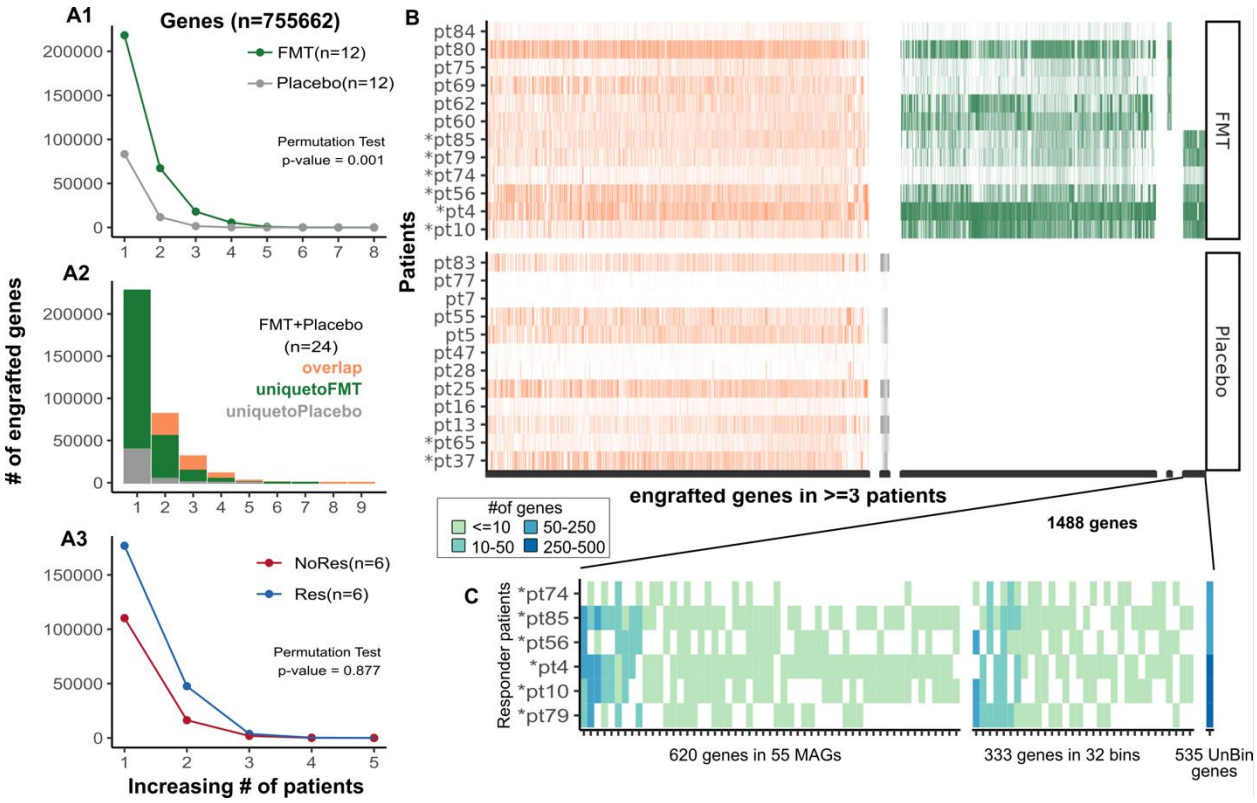

Figure 4. **Identifying genes commonly engrafted in FMT responders. A.** Counts of apparently engrafted genes in FMT and placebo groups. **A1.** Examination of apparently engrafted genes in patients receiving FMT (n=12) or placebo (n=12) treatment. The x-axis shows the number of patients in which each gene appears to be engrafted, emphasizing common gene engraftment. **A2.** Discriminating donor gene engraftment patterns across all patients (n=24) to distinguish unique engraftment in FMT (green), in Placebo (grey), and genes engrafted in both FMT and Placebo (orange). **A3.** Comparison of apparently engrafted genes in FMT patients in responders (n=6, blue) and non-responders (n=6, red). The differences between the points on the green and grey lines (A1) or blue and red lines (A3) were used to calculate the test statistics for the permutation tests. **B.** Donor genes that engrafted in at least 3 patients are categorized as follows: genes engrafted in FMT patients but also present in the placebo group are shown in orange; genes unique to the placebo or FMT groups are depicted in grey and green, respectively. Among genes apparently engrafted only in FMT, those found in both responders and non-responders, as well as those unique to each group, are separately grouped on the x-axis. **C.** Location of the 1,488 genes apparently uniquely engrafted in 3 or more FMT responders in our Donor B assemblies. Among the 1,488 genes, 333 were found in 32 metagenomic bins, 620 were present in 55 MAGs, and 535 genes were located on un-binned contigs ("UnBin").

To enrich for legitimate engraftment events, we focused on genes engrafted in three or more patients. This provided a set of 45,419 genes. Among these, 56.9% (25,826) were engrafted in FMT recipients and also present in at least one placebo recipient. Notably, 37.9% (17,230) were exclusive to FMT recipients, while only 5.2% (2,363) were unique to the placebo group. This final category, since it is known to be false positives, was not subject to further analysis. Genes unique to responders represented 3.3% (1,488), compared to only 0.6% (283) in non-responders (**Figure 4B**). To trace the origins of genes uniquely associated with FMT responders, we examined their presence in contigs grouped in MAGs and non-MAG bins. We found 620 genes within 55 unique

MAGs, 535 in contigs not assigned to any bin ("UnBin"), and 333 in 32 non-MAG bins (**Figure 4C**). These findings highlight the importance of our gene-based approach. Relying solely on genome detection strategies using MAGs would have prevented the identification of most of these genes.

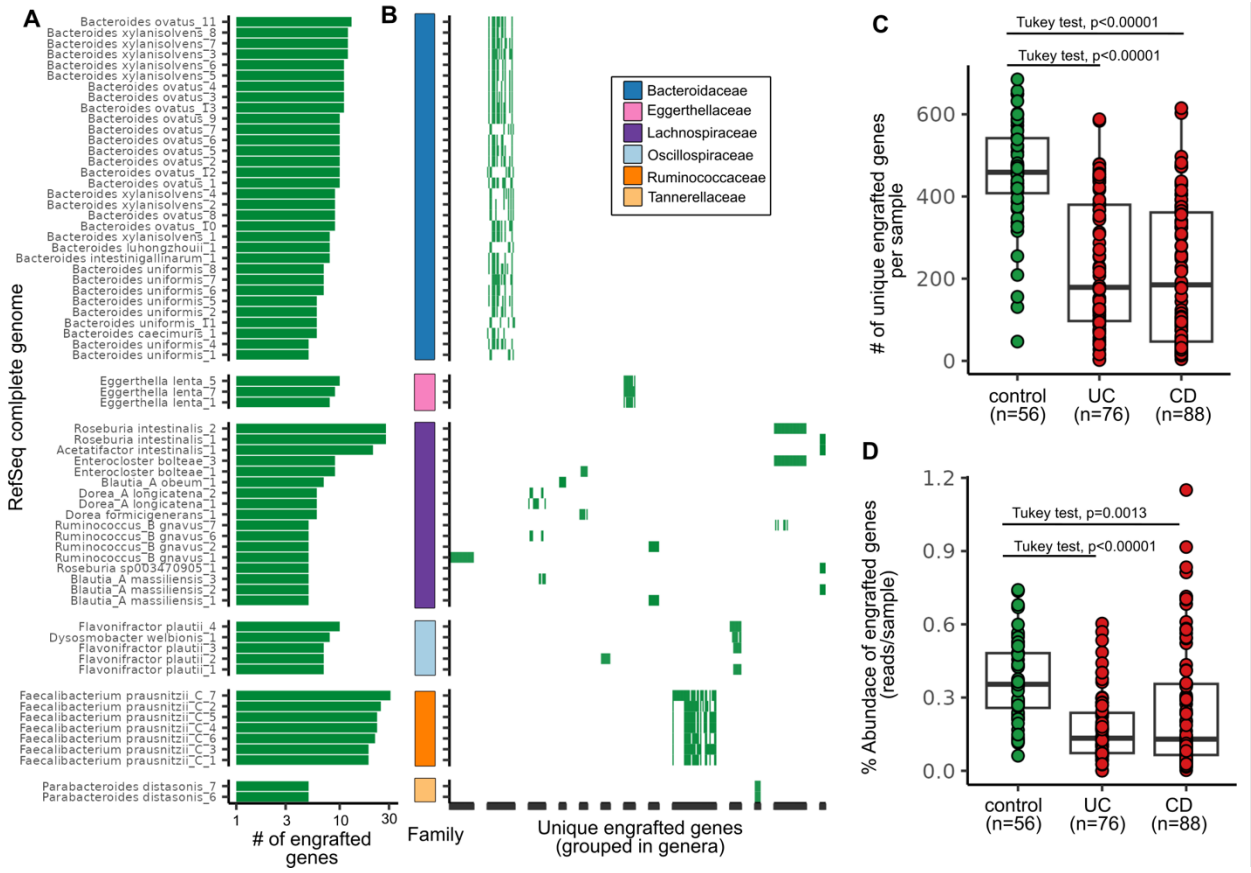

Figure 5.**Commonly engrafted genes in FMT responders are strain-specific and depleted in IBD patients. A.** We searched for genes commonly apparently engrafted in FMT responders in the RefSeq complete bacterial genomes (n=33,167) database. The number of observed engrafted genes per genome is represented by green bars on the x-axis, while strains with at least 5 engrafted genes are displayed on the y-axis. Bacterial strains are grouped and color-coded on the y-axis according to their family. **B.** To demonstrate the specificity of these genes within a genus, unique engrafted genes are represented on the x-axis and compared across the genomes depicted on the y-axis (shared with panel A). **C.** Comparison of the number of genes commonly engrafted in responders that were found in healthy individuals (n=56) and patients with UC (n=76) and CD (n=CD). We utilized metagenomic reads from a publicly available dataset (PRJNA40007229[33]) that includes samples from healthy donors and IBD patients to explore the association of these genes with health status. **D.** Comparison of the relative abundance of these commonly engrafted genes within the same cohort as panel C.

Characterizing a strain collection with commonly engrafted genes depleted in IBD patients.

To further investigate the 1,488 genes engrafted in at least 3 responders, we searched for these genes in 33,167 RefSeq genomes from all bacterial phyla, updated as of May 2023. Our objective was to ascertain whether these genes are widely distributed across various taxa, or are specific to certain strains.

Our analysis revealed that 66 out of the 33,167 genomes contained the genes of interest, each with more than five genes per genome. These genomes were distributed across six bacterial families (**Figure 5A**). Notably, genes identified in the families *Bacteroidaceae* were present in multiple species within their genera, suggesting these were widely shared between strains within the *Bacteroides* genus. By contrast, genes present in *Lachnospiraceae* and *Ruminococcaceae*, were more strain-specific within a species. The remaining families contained 11% of the detected genes. (**Figure 5B**).

Among the 1,488 genes identified, 1,415 were annotated as coding sequences (CDS) with a median length of 491 bp. Of these, 845 proteins were previously characterized or had predicted function by homology, while the remaining were hypothetical proteins with no predicted function. Among the characterized proteins, 593 were distributed across 19 diverse Clusters of Orthologous Groups (COG) categories. The most prevalent categories included Transcription, which accounted for 12.8% of these proteins, followed by Replication, Recombination, and Repair (12.3%), and Carbohydrate Transport and Metabolism (8%).

One notable observation (**Supp Figure 3**) is that for any individual only a small portion of the microbiome features are shared between patient and donor. However, most of the donor's microbiome features are shared with at least one subject. This is also true of engrafted features. This reflects the high individual variability in human gut microbiomes.

Expanding our investigation, we utilized a larger dataset of publicly available metagenomic samples (PRJNA40007229[33]), which included healthy individuals (n=56), UC patients (n=76), and

339 patients with Crohn's disease (CD) (n=88). We mapped these reads to the 1,488 genes to
340 determine their presence and relative abundance in the samples. Intriguingly, we found a notable
341 reduction in both the number and relative abundance of these genes in IBD patients compared
342 to healthy individuals. (Tukey test, p-values in **Figure 5C and 5D**, overall ANOVA p-values
343 <0.0001). These observations, derived from an independent and more extensive dataset, further
344 underscore the potential significance of these genes in the context of IBD.
345

346 ## Discussion
347
348 FMT has emerged as a promising therapeutic option for UC, demonstrating efficacy in RCTs when
349 compared to placebo[13,34]. However, the variability in patient response remains a critical
350 challenge, underscoring the need to elucidate the factors influencing the success of FMT. Donor
351 microbiota composition has been implicated in treatment outcomes, with studies reporting both
352 donor-dependent efficacy and the benefits of pooling microbiomes from multiple donors[5,18,35].
353 In this study, we aimed to dissect the mechanisms underlying successful FMT by examining
354 microbial engraftment in UC patients. We examined the rates of apparent engraftment in both
355 FMT and placebo groups. We observe a significant level of spurious engraftment (false-positives)
356 in the placebo group which confounds the prediction of true engraftment. Additionally, our data
357 suggest that analyzing engraftment across multiple patients from a single donor enhances the
358 accuracy of detection. Finally, we applied a gene-based strategy for engraftment analysis, which
359 addresses several limitations inherent in read-based and MAG focused approaches, offering a
360 refined approach to understanding and improving FMT outcomes.
361
362 Our analysis also underscores the necessity of integrating placebo group sequencing in
363 investigation of post-FMT engraftment. Our data from the placebo controls demonstrated that a
364 substantial amount of false positives detection occurs, and caution must be taken when
365 interpreting results. These false-positives arise because donor features in a patient (e.g.
366 species/strains/MAGs/genes) may be present at baseline but below the level of detection. If
367 these features increase and are detected at a second timepoint, then they will appear to be

368 engrafted. By refining engraftment thresholds and employing rigorous controls, we aim to
369 provide a clearer and more reliable framework for interpreting FMT outcomes in UC.
370
371 The application of MAGs in studying microbial engraftment after FMT presents significant
372 challenges. The inherent difficulties in accurately assembling MAGs from complex microbial
373 communities result in the exclusion of a substantial portion of sequencing data. The non-MAG
374 metagenomic data will include species present at lower abundance, plasmids, mobile genetic
375 elements, and when multiple strains of a species are present - strain-specific genes. Using the
376 define thresholds for donor MAG presence and absence in subjects, we observed 4 MAGs
377 predicted to be engrafted in at least three FMT recipients, but only one of these, a
378 *Lachnospiraceae*, was shared between 3 responders (*Hominisplanchenecus faecis*).
379
380 The clearest signals of engraftment in our study came from the gene dataset where specific sets
381 of donor genes were predicted to be engrafted and associated with response in multiple FMT
382 recipients. The gene-level analysis is consistent with most engraftment events being associated
383 with strain displacement where a donor strain replaces a recipient strain of the same species.
384 Here we use strain in the context of the presence and absence of accessory genes which focuses
385 on functional differences between strains. Strains can be defined by single nucleotide
386 polymorphisms in core genes (e.g. StrainPhlAn) which is a powerful approach for evolutionary
387 studies but does not directly identify functional differences between strains. Approximately 60%
388 of these genes were not found in MAGs even though our culture-enriched metagenomic
389 increased the number of MAGS 4-fold and increased the size of most MAGs compared to
390 standard metagenomics. Furthermore, MAGs containing these genes (n=55) were not predicted
391 to be engrafted. This reflects the incomplete nature of MAGs and the challenges of establishing
392 the thresholds set for presence and absence of features (**Supp Figure 1**).
393
394 Using a gene-centric methodology we identified specific sets of genes uniquely present in
395 patients who responded to FMT treatment. Many of these genes are involved in diverse microbial
396 metabolic pathways. However, a main challenge in interpreting these results arises from the

397 limited annotations available in existing databases, and a significant proportion of the predicted
398 genes (~25%) have no predicted function. Our study was limited by small number of subjects and
399 responders in our trial. Despite these limitations, when examining these commonly engrafted
400 genes with a larger cohort of IBD patients, we found that they were consistently depleted,
401 suggesting a possible protective or beneficial role for these genes that is disrupted in this disease
402 state.
403
404 Our analysis revealed a notable pattern of strain specificity among these genes, particularly in
405 species within the *Lachnospiraceae* and *Ruminococcaceae* families. This specificity suggests that
406 certain strains of these species may be important for achieving the desired therapeutic outcomes
407 of FMT. Conversely, in the *Bacteroides* genus, we observed that these genes are not confined to
408 strains of specific species but are rather widespread across the genus (**Figure 5**). As might be
409 predicted from this distribution, there is relatively low level of prediction for *Bacteroides* MAG
410 engraftment (**Figure 3**). This distribution pattern could indicate a broader functional role for
411 these genes within the *Bacteroides*, or may be reflective of an accessory genome that is more
412 widely shared across the family.
413
414 Strain level engraftment may also reflect direct strain-strain competition where donor strains
415 that are more adept at outcompeting a patient's own strains that may be independent of
416 response to FMT. However, we do find specific donor genes engrafted in multiple responders,
417 and also show these genes are depleted in stool metagenomic samples from ulcerative colitis
418 and Crohn's disease patients compared to healthy controls (**Figure 5C,D**). These observations
419 provide support for a role of these genes in response to FMT.
420
421 The differential distribution of engrafted genes between taxa such as *Lachnospiraceae*,
422 *Ruminococcaceae*, and *Bacteroides* underscores the complex interplay of microbial dynamics in
423 FMT. It highlights the importance of understanding specific microbial contributions to host
424 health, which can lead to more targeted and effective microbial therapies. A consortium of
425 strains defined by gene-level engraftment might be more effective as a FMT alternative than a

426 consortia based only on species considerations. By focusing on these key microbial players and
427 their functional genes, and investigating their roles in health and disease, we can begin to piece
428 together the intricate mechanisms through which the microbiota exerts their beneficial effects,
429 paving the way for refined FMT strategies tailored to individual microbial compositions.
430
431

432 Methods

433

434 Study design and sample collection.

435

436 The study design and sample collection was as described previously[5]. Briefly, 70 active UC
437 patients (Mayo score >=4 with an endoscopic Mayo score >=1) were randomly assigned to either
438 6 weeks of FMT (once per week; 50 mL, via enema, from healthy anonymous donor) or placebo
439 (once per week; 50 mL water enema) in a double-blind randomized controlled trial. Stool samples
440 were collected at baseline (before treatment), and during each week of the trial.
441

442 DNA extraction and 16S rRNA gene sequencing

443

444 Genomic DNA extraction and PCR amplification of the V3 region of 16S rRNA gene was conducted
445 using previously described protocols[5,40,41]. Briefly, 0.2 g of fecal matter was mechanically
446 homogenized using ceramic beads in 800 µL of 200 mM NaPO 4 (pH 8) and 100 µL of guanidine
447 thiocyanate-EDTA-N-lauroyl sacosine. This was followed by enzymatic lysis of the supernatant
448 using 50 µL of 100 mg/mL lysozyme, 50 µL of 10 U/µL mutanolysin, and 10 µL of 10 mg/mL RNase
449 A for one hour at 37 °C. Then, 25 µL of 25% sodium dodecyl sulfate (SDS), 25µL of 20 mg/mL
450 proteinase K, and 75 µL of 5 M NaCl was added, and incubated for one hour at 65 ºC.
451 Supernatants were collected and purified through the addition of phenolchloroform-isoamyl
452 alcohol (25:24:1; Sigma, St. Louis, MO, USA). DNA was recovered using the DNA Clean &
453 Concentrator TM -25 columns, as per manufacturer's instructions (Zymo, Irvine, CA, USA) and
454 quantified using the NanoDrop (Thermofisher, Burlington, ON). After genomic DNA extraction,
455 the V3 region of the 16S rRNA gene was amplified via PCR using these conditions per reaction
456 well: Total polymerase chain reaction volume of 50 µL (5 µL of 10X buffer, 1.5 µL of 50mM MgCl
457 2 , 1 µL of 10 mM dNTPs, 2 µL of 10mg/mL BSA, 5 µL of 1 µM of each primer, 0.25 µL of Taq
458 polymerase (1.25U/ µL), and 30.25 µL of dH 2 O. Each reaction was divided into triplicate for
459 greater efficiency. The primers used in this study were developed by Bartram et al.,2011. PCR
460 conditions used included an initial denaturation at 94 ºC for 2 minutes, followed by 30 cycles of
461 94 ºC for 30s, 50 ºC for 30s, 72 ºC for 30s, followed by a final elongation at 72 ºC for 10 minutes.
462 All samples were sequenced using an Illumina MiSeq platform at the McMaster Genomics Facility
463 (Hamilton, Ontario, Canada). Samples were processed in batches, meaning not all samples were
464 extracted and sequenced at the same time.
465

466

467 ## 16S rRNA gene sequencing processing pipeline

468

469 Cutadapt[42] v1.14 was used to filter and trim adapter sequences and PCR primers from the raw
470 reads, using a quality score cut-off of 30 and a minimum read length of 100 bp. We used DADA2[28]
471 v1.14.0 to resolve the sequence variants from the trimmed raw reads as follow. DNA sequences
472 were trimmed and filtered based on the quality of the reads for each Illumina run separately. The
473 Illumina sequencing error rates were detected, and sequences were denoised to produce ASV
474 count table. The sequence variant tables from the different Illumina runs were merged to
475 produce a single ASV table. Chimeras were removed and taxonomy was assigned using the
476 DADA2 implementation of the RDP classifier against the SILVA database[43] v1.3.2, at 50%
477 bootstrap confidence.

478

479 The ASV, taxonomy, and clinical tables were all merged into one data object in R v4.2.0 using
480 Phyloseq v1.40.0 package[44].

481

482 ## Library preparation for shotgun metagenomic sequencing.

483

484 We conducted direct shotgun metagenomic sequencing on 48 samples collected from 24 patients
485 (12 patients who received FMT (6 responders and 6 non-responders) and 12 who received
486 placebo (both responders and 10 non-responders)), at 2 time points each (baseline and 6 weeks
487 after treatment), as well as 4 samples from Donor B. Genomic DNA was standardized to 5 ng/µL
488 and sonicated to 500 bp. Using the NEBNext Multiplex Oligos for Illumina kit (New England
489 Biolabs), DNA ends were blunted, adapter ligated, PCR amplified, and cleaned as per
490 manufacturer's instructions. Library preparations were sent to the McMaster Genome Facility
491 and sequenced using the Illumina HiSeq platform, with a mean depth of approximately 18 million
492 paired-end reads per sample.

493

494

495 ## Culture-enriched and independent metagenomics on Donor B samples

496

497 A fresh, anaerobic fecal sample was collected from Donor B. The collected sample was cultured
498 using 33 different media, and incubation of plates anaerobically and aerobically resulted in 66
499 culture conditions for culture-enriched molecular profiling using a previously described
500 protocol[22]. The list of media and culture conditions are described therein. 16S rRNA gene
501 amplicon sequencing was conducted on plate pools of all 66 culture conditions. To determine a
502 subset of plates that adequately represent the sample, the distribution of ASVs in the direct
503 sequencing was compared to the culture-enriched sequencing using the PLCA algorithm[25].
504 Shotgun metagenomics was conducted on the 13 plate pools identified by the PLCA algorithm as
505 representing the community. Genomic DNA was isolated from the all 13 selected plate pools and
506 shotgun metagenomics conducted as previously described, with a mean depth of approximately
507 14 million paired-end reads per plate pool. Direct shotgun metagenomics was also conducted on
508 the same fecal sample directly.

509

510 ## Comparison of the culture-enriched metagenomics with direct metagenomics data

511

512 To build a culture-enriched metagenomic library, raw shotgun sequences from the selected plate
513 pools and the original fecal sample collected from Donor B for culturing were co-assembled as
514 follows: Low-quality reads and sequencing primers were removed using Trimmomatic[45] v0.38
515 with 'LEADING:3 TRAILING:3 SLIDINGWINDOW:4:15 MINLEN:36' option. The reads were
516 decontaminated for any human DNA using DeconSeq[46] v0.4.3. These cleaned reads were then
517 co-assembled using metaSPAde[47] v3.10.1. Filtered raw reads were mapped to contigs (minimum
518 length of 2.5 kb) using BWA-mem[48] v0.7.17, and then binned with Metabat2[49] v2021. This was
519 done for both the CEMG assembly and direct metagenomic sequencing (DMG) reads from the
520 fecal sample, using identical methods. These datasets are referred to as CEMG and DMG,
521 respectively.

522

523 The microbial compositions of DMG and CEMG datasets were then comprehensively evaluated
524 using the following procedure: The single-copy core genes were identified within each bin using
525 CheckM[50] v1.1.2, any bin with minimum 70% completion and maximum 10% contamination was
526 defined as a metagenome assembled genome (MAG). The shotgun reads were mapped to the
527 assembled contigs to estimate sequence coverage for all contigs, Bins, and MAGs. We used BWA-
528 mem[48] to map reads to assembled contigs and the anvio pipeline[51] to normalize the coverage to
529 depth of sequencing. Detection values were calculated for each bin using anvio[51]. A detection
530 value is defined as the proportion of a given MAG that is covered by at least one read; in other
531 words, it estimates the proportion of MAG that recruited reads to it.

532

533 For taxonomic assignment of the metagenome-assembled genomes (MAGs), we utilized GTDB-
534 Tk[52] v202.0. We built a maximum-likelihood phylogenetic tree using the aligned protein
535 sequences from GTDB with FastTree[53]. To compare the lengths of MAGs in DMG and CEMG, we
536 selected MAGs based on their proximity in the phylogenetic tree. The total assembly length was
537 determined by summing contig lengths, calculated with metaSPADE, in R. All figures were created
538 and visualized using R version 4.0.3.

539

540 ## Shotgun metagenomic sequencing processing pipeline

541

542 Raw reads were filtered to remove low-quality sequences and decontaminate human-derived
543 reads using KneadData. These filtered reads were then analyzed to identify species- and strain-
544 level markers with MetaPhlAn4 and StrainPhlAn4, respectively. To profile the relative abundance
545 of species, MetaPhlAn4[29] v4.0.4 was employed with the '-t rel_ab' option. Similarly, for strain
546 tracking, the '-t marker_ab_table' option was used, alongside the '--nreads' parameter to specify
547 the number of metagenomic reads. A default minimum Reads Per Kilobase (RPK) of 1 was used
548 to identify a marker as present.

549

550 Filtered metagenomic reads from donor samples (n=4) and culture-enriched plate pools (n=13)
551 were co-assembled using metaSPAdes[47] v3.10.1 to create a comprehensive Donor B database.

552 Contigs of at least 2.5 kb were annotated with Bakta[54] v1.5.0 to identify genes. These annotated
553 contigs were then binned with Metabat2[49] v2021, leveraging mapping data from all plate pools
554 and Donor B samples. The quality of the resulting bins was evaluated using CheckM[50] v1.1.2; bins
555 with a completion rate of at least 70% and contamination of 10% or less were designated as
556 metagenome-assembled genomes (MAGs). Taxonomic classification of MAGs was performed
557 using GTDB-Tk[52] v202.0.
558
559 All patient metagenomic samples (n=48) were normalized to the lowest sequencing depth
560 observed in the dataset (5.5 million paired-end reads) using seqtk[55] v1.1.0 for random
561 subsampling. These rarefied reads were mapped to the genes and contigs assembled from Donor
562 B using BWA-mem[48] v0.7.17, applying perfect match filtering options '-O 60 -E 10 -L 100'.
563 Coverage information at 1x was calculated using samtools[56] 'coverage'.
564
565 A database of 33,167 RefSeq bacterial genomes, categorized as 'assembly-level complete' and
566 downloaded as of May 2023, was compiled using a custom Python script. We identified a unique
567 set of genes present exclusively in responder patients and used these as query sequences for
568 BLAST searches against this database, employing BLAST[57] v2.13.0+. Hits were selected based on
569 stringent criteria: percent identity of at least 90%, query coverage of at least 90%, and gene
570 lengths of 100 base pairs or more. Genomes containing at least five such genes were visualized.
571 The taxonomy of these genomes was determined using GTDB-Tk[52] v202.0. To functionally
572 annotate these genes, they were clustered at 90% protein identity using MMseqs2[58] v13.45111
573 and then profiled against KEGG, COG, and PFAM databases using eggNOG-mapper[59] v 2.1.7 and
574 database version of 5.0.2.
575
576 Additionally, a publicly available metagenomic dataset (PRJNA40007229[33]), comprising samples
577 from 56 healthy subjects, 76 patients with ulcerative colitis (UC), and 88 patients with Crohn's
578 disease (CD), was downloaded from the Sequence Read Archive (SRA). These samples were
579 mapped to the identified gene set using BWA-mem[48] v0.7.17, applying strict matching filters ('-O
580 60 -E 10 -L 100'). samtools[56] 'coverage' was then used to quantify the presence of these genes in
581 each sample and to calculate the percentage of reads mapped to these genes per sample.
582
583
584 ## Feature Types
585
586 As described above, we used the 16S and shotgun metagenomic reads from our samples to
587 generate five datasets, each consisting of a single feature type: 16S rRNA gene amplicon ASVs,
588 species, strains, MAGs, and genes. The 16S ASVs are the only feature type that was generated
589 using amplicon-based methods. The rest were based on the shotgun metagenomic reads. Within
590 these remaining four, species and strains were read-based methods because they did not require
591 assembly, while MAGs and genes were assembly-based, since they used contigs of assembled
592 reads. We analyzed all five feature types to determine which method allowed us to minimize the
593 spurious appearance of engraftment, while still having the sensitivity to detect true engraftment
594 that may be happening.
595

Assessing Engraftment

In order for us to call a feature "apparently engrafted", it needed to meet three criteria: 1. It must be observed in the Donor B samples. 2. It must be absent from the patient's pre-treatment sample. 3. It must be present in the patient's post-treatment sample.

For all feature types, criterion 1 was met if the feature was observed at least once in any Donor B sample. The definitions of criteria 2 and 3 (absence and presence) depended on feature type. Our aim was to be quite strict with these criteria in order to minimize spurious identification of engraftment.

For the 16S ASV, strain, and species feature types, a feature was deemed to be absent at baseline (criterion 2) if the patient's pre-treatment sample contained that feature exactly 0 times. Even a single read assigned to a given feature in a baseline sample would remove it from consideration for engraftment in that patient. Criterion 3 (presence after treatment) was met if the feature's relative abundance in the post-treatment sample surpassed a given threshold. The threshold varied between the three feature types, and in each case was chosen such that, when it was applied to Donor B's own samples, it eliminated the bottom 20% of features from the merged datasets. The cutoffs were 1.3e04 for 16S ASVs and strains, and 0.0072 for species. **Supp Figure 1** shows the presence vs. relative abundance histograms used to determine these cutoffs.

For assembly-based feature types (genes and MAGs), presence and absence were determined by 1x coverage, rather than abundance. In order to identify reasonable cutoffs for MAGs, we mapped Donor B's reads back to the database of Donor B assemblies, and then created a histogram showing the frequencies with which MAGs were covered at least 1x over different proportions of their length. We observed a u-shape in this histogram, where approximately 50% of the MAGs in each sample were covered 1x over at least 75% of their length, most intermediate values of coverage were present at very low frequency, and there was another peak of varying height starting at 1x coverage over less than 20% of the MAG's length. We reason that MAGs that were present in a given sample are represented by the peak above 75% coverage, while MAGs that are absent from that sample can be seen in the lower peak. We called a MAG absent in a baseline sample if it was covered at least 1x over less than 20% of its length, and present in a post-treatment sample if it was covered at least 1x over at least 75% of its length. For genes, we used a 25% coverage criterion to define a gene as absent, and required its 1x coverage to be over at least 90% of its length in order to call it present after treatment. Both cutoffs were raised relative to the MAG cutoffs to allow for the fact that different genes which happen to share similar motifs can have quite similar DNA sequences over a substantial proportion of their lengths.

Within each patient, any features that failed to meet even one of the three criteria were removed from consideration for engraftment.

Statistical Analysis of Engraftment

Once apparently engrafted features were identified in all samples across all feature types, we sought to test whether patients who received FMT had higher levels of apparent engraftment than those who received placebo treatment. We constructed three test statistics, all of which we tested using the same permutation test. These three test statistics were the differences between FMT and placebo groups in: 1. the number of features engrafted at least once in the given treatment group (T_1), 2. the number of engraftment events in that occurred in each treatment group (i.e. the count of engrafted features, weighted by the number of patients each feature was engrafted in) (T_2), and 3. the number of engraftment events weighted by the number of patients each event occurred in (.e. the count of engrafted features, weighted by the square of the number of patients each feature was engrafted in) (T_3). The reason for this third test statistic was that we reasoned that a feature that appears engrafted in multiple patients is less likely to have been a spurious signal of engraftment, and so we wanted to up-weight those features based on the number of individuals they were engrafted in. Looking at the graphs in **Figure 2 (A1, B1, C1), 4(A1), and 5(A1**), the test statistics can be calculated as follows, where x is the number of patients a feature is engrafted in, and f(x) is the number of features engrafted in exactly that many patients:

$$T_1 = \sum \left(f_{FMT}(x) - f_{placebo}(x) \right) \quad (1)$$

$$T_2 = \sum x \left(f_{FMT}(x) - f_{placebo}(x) \right) \quad (2)$$

$$T_3 = \sum x^2 (f_{FMT}(x) - f_{placebo}(x)) \quad (3)$$

Permutation tests were conducted by permuting the group membership of each patient 1,999 times, and for each permutation calculating the number of engrafted features, engraftment events, and weighted engraftment events in each group, and taking their difference. The 2,000th value in each permuted null distribution was the observed value. Two-tailed p-values were calculated by finding the quantile of the observed test statistic in the null distribution, taking its distance from 0 or 1, whichever was smaller, and doubling that value. This same method was used to compare the amounts of apparent engraftment in responder- vs. non-responder-patients within the FMT treatment group **(Figure 2(A3, B3, C3), 4(A3), and 5(A3)).**

Once count tables or coverage values had been calculated for a given feature type, all data organization and analysis code were written in R v4.2.0 using the tidyverse[60] collection of packages. Figures were generated in R using ggplot2 and tidytext and refined in Inkscape. R scripts are available at https://github.com/SShekarriz/UCFMT1.

Acknowledgements

This work was supported by grants from Crohn's Colitis Canada, and the Inflammation, Microbiome, and Alimentation: Gastrointestinal and Neuropsychiatric Effects (IMAGINE) Network CIHR grant. M.G.S. is supported by a Canada Research Chair. During some of this work S.S. was supported by Mitacs Elevate Fellowship and F.J. Whelan was supported by an Anne McLaren Fellow funded by the University of Nottingham and a Marie Skłodowska-Curie Individual Fellowship (grant agreement number 793818). The authors would like to thank Dr. Ben Bolker and the McMaster biodata lunch group, as well as Dr. Kevin Purbhoo, for their valuable insight and suggestions in the development of our statistical methods.

Supplementary Results

Culture-enriched metagenomics improves the quality of de novo assembly and taxonomic binning.

It is often challenging to determine if the donor is responsible for the observed microbial changes after FMT or if they instead represent population restructuring within the patient's own microbiota. Assembly-based metagenomic approaches provide better resolution, and may be more suitable than amplicon- or read-based metagenomic techniques for tracking strain- or gene-level changes. However, the quality of genome assembly and taxonomic binning of metagenomic assemblies can be poor[56] and recovering low-abundance taxa is challenging[37]. Previous studies have shown that the human microbiota is culturable[22,24,25,38], and that a combination of direct (culture-independent) sequencing and sequencing after comprehensive culturing can result in increased observed microbial diversity[22,25,39].

We hypothesized that co-assembling sequences from direct and culture-enriched metagenomic sequencing (CEMG) of the Donor B microbiota would improve gene and metagenome assembled genome (MAG) recovery from this donor compared to the commonly used direct metagenomic (DMG) approach. To test this hypothesis, we conducted shotgun metagenomic sequencing on a previously cultured[22] fecal sample from Donor B (**Figure 1**). We then compared the assemblies and microbial binning qualities achieved from DMG vs CEMG sequencing for this single fecal sample.

DMG resulted in 35,577 assembled contigs (> 2.5 Kb) accounting for ~340 Mb of the assembled sequences, whereas the same number of contigs in CEMG captured ~620 Mb. In addition to providing more contigs, the CEMG method produced longer contigs, specifically (**Supp Figure 2A**). These longer contigs enhanced gene predictions and generated more (132 vs. 49) metagenome-assembled genomes (MAGs; > 70% complete and < 10% contamination; see Methods). To assess the specificity of the two approaches, we mapped raw reads from both DMG and CEMG to the

720 assembled MAGs from both assemblies. CEMG provided 83 more MAGs than DMG; however,
721 most of these additional MAGs were well covered by the DMG reads, indicating that their
722 presence is not due to contamination, but instead increased representation in the sequencing
723 (**Supp Figure 2B**). The additional MAGs from CEMG sequencing are not derived from any
724 particular taxonomic groups, but instead represent multiple families in proportion to their
725 abundance in the DMG approach (**Supp Figure 2B, C**).
726
727 To examine the quality of assembled MAGs, we selected 40 homologous MAGs from the DMG
728 and CEMG assemblies based on their position in a maximum-likelihood phylogenetic tree of core
729 genome alignment (data not shown), and compared their genome sizes. We found that 24 out of
730 the 40 MAGs (60%) were longer in the CEMG assemblies than in DMG (**Supp Figure 2D**). We
731 concluded that CEMG sequencing enhances the assembly of genes and MAGs for intestinal
732 microbiota and set to use this approach to investigate microbial engraftment following FMT.
733
734

Supplementary Figures

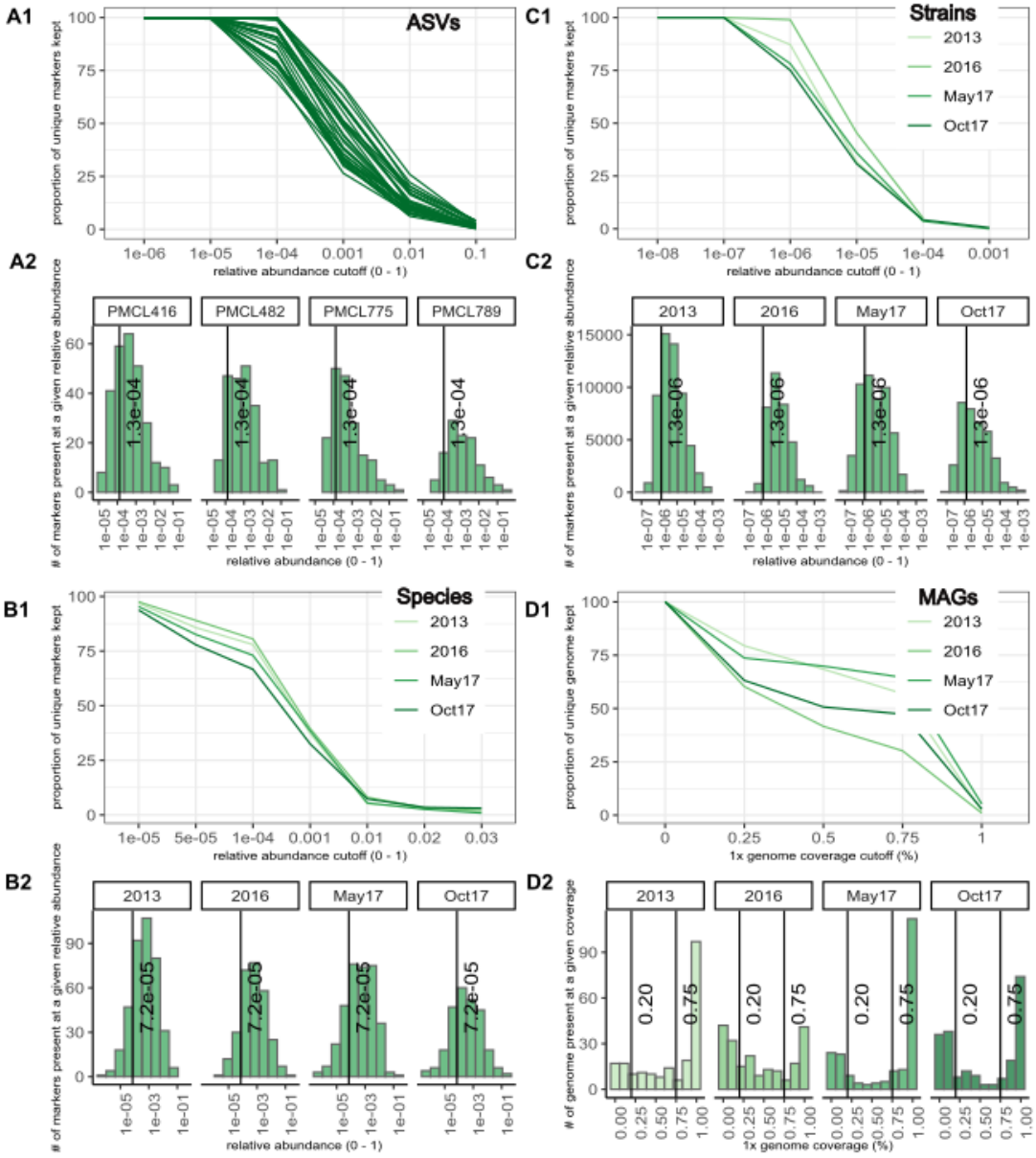

Supp Figure 1. **Profiles of features in Donor B samples, for determining engraftment cutoffs.** *Panels (A – D)1 show the proportion of unique features retained (y-axis) after all features below a given cutoff (x-axis) are removed. In panels A (16S ASVs), B (species markers), and C (strain markers), the cutoffs are relative abundances. In panel D (MAGs), the cutoffs are the proportion of the genome covered by at least one read. Panels (A – D)2 are histograms of the frequencies of various relative abundances (A – C) or 1x coverages (D). Vertical black lines in A2, B2, and C2 show our chosen cutoffs to define a feature as present, in both cases removing the bottom 20% of the density of the histogram. Vertical black lines in D2 show our chosen cutoffs for both absence and presence, removing the distributions' two peaks as described in the Methods section.*

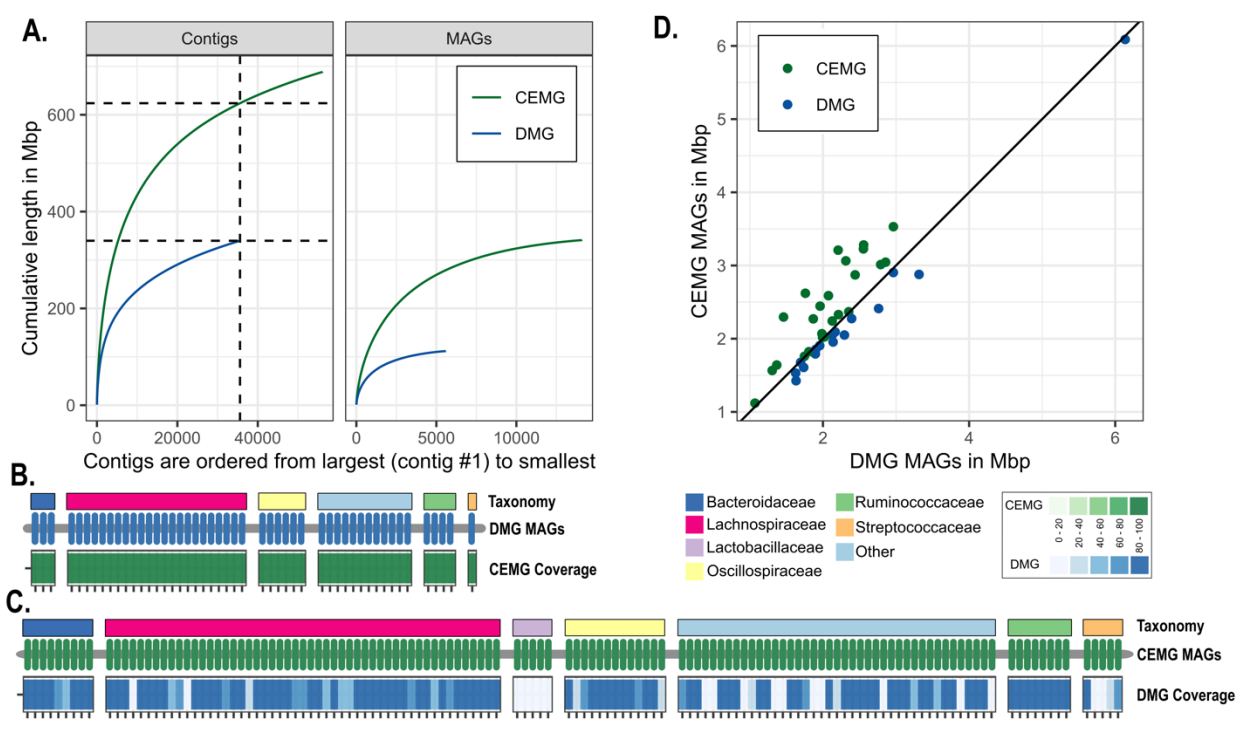

Supp Figure 2 **Comparison of culture enriched (CEMG) and direct metagenomics (DMG) for Donor B. A.** The cumulative lengths of assembled contigs >2.5 kb for all contigs, and for contigs belonging to MAGs. Vertical dashed line represents the number of contigs in the DMG assembly, horizontal lines represent the total assembly size at that number of contigs for DMG and CEMG respectively. B. DMG and CEMG read mapping coverage (mean MAG coverage at least 1X) of the MAGs (n=49) assembled via DMG. The top colour bar shows the family-level taxonomy of the MAGs. C. CEMG and DMG read mapping coverage for the MAGs (n=132) assembled via CEMG. D. Genome sizes among homologous MAGs in CEMG and DMG.

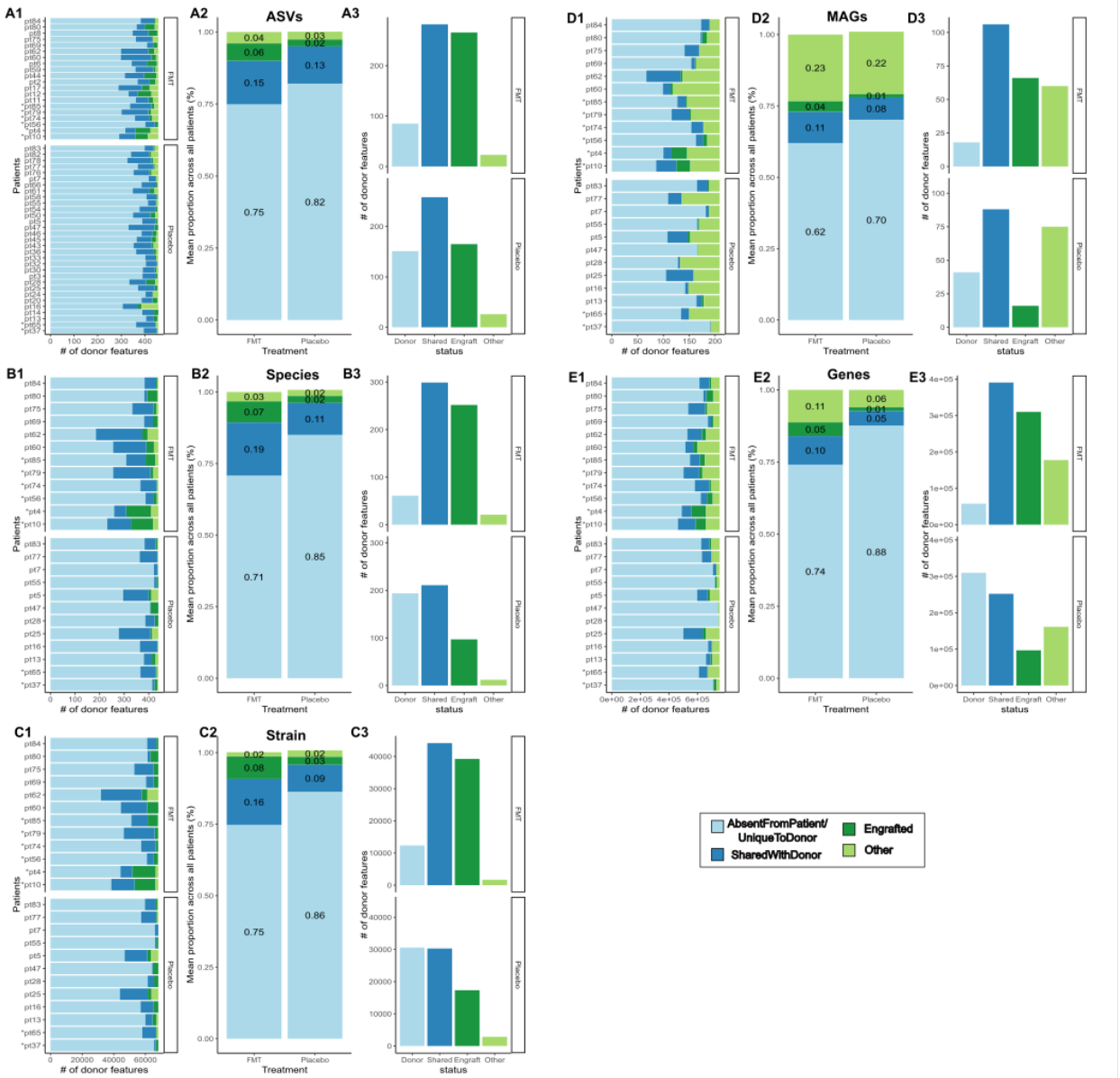

Supp Figure 3 **Proportion of Donor B's features that are engrafted, shared between donor and recipient, or only found in donor.** Panels A(1 – 3) concern the ASV feature type, panels B(1 – 3) concern the strain feature type, panels C(1 – 3) concern the species feature type, panels D(1 – 3) concern the MAG feature type, and panels E(1 – 3) concern the gene feature type. Panels (A – E)1: For each patient, we calculated the proportion of Donor B features of a given feature type that were absent (as defined by the absence cutoff of our engraftment criteria) from both the pre- and post-treatment samples (light blue: Donor), were already present (as defined by our presence cutoff ditto) in the pre-treatment sample (dark blue: Shared), met the criteria for engraftment (dark green: Engraft), or did not meet any of these criteria (light green: Other). In almost every case, the majority of Donor B's features were absent from the patient, and the 'Other' category contained the fewest features. Panels (A – E)2: the mean values of the categories in (A – E)1 across all patients within a given feature type. Again showing that, within any individual patient, most Donor B features are absent from that patient at all times. Panels (A – E)3: Taking all patients in a given treatment arm (FMT or Placebo) together, features are counted in the light blue (Donor) category if they are absent from both timepoint samples from **all** patients. Features are counted in the Shared (dark blue) and Engraft (dark green) categories if they meet the corresponding above-define criteria in **any** patient (meaning some features may be counted in both categories). Features that do not meet any of the above criteria are included in the Other (light green) bar. In all cases, the Donor category contains more features in the Placebo group than the FMT group; however, the gene feature type shows the largest proportional difference. In all cases, the

FMT group includes more Engraft features than the Placebo group. The MAG and gene features types show the largest proportional difference.

Supplementary Tables

Supplementary Table 1: Permutation-test p-values for all three test statistics.[1]

Feature Type	Test	T_1 p-value	T_2 p-value	T_3 p-value
16S	FMT vs Placebo	<0.0005	<0.0005	<0.0005
	Responders vs Non	0.961	0.957	0.996
species	FMT vs Placebo	0.025	0.021	0.014
	Responders vs Non	0.323	0.336	0.357
strain	FMT vs Placebo	0.01	0.005	0.005
	Responders vs Non	0.296	0.29	0.296
MAG	FMT vs Placebo	0.007	0.01	0.008
	Responders vs Non	0.176	0.189	0.239
gene	FMT vs Placebo	0.001	0.001	0.001
	Responders vs Non	0.87	0.879	0.877

[1] P-values for the three test statistics were not identical within each dataset, but were similar. P-values < 0.05 are highlighted in blue. All the FMT vs. Placebo tests were statistically significant, while none of the FMT Responder vs. Non-Responder tests were. In only one case (highlighted in yellow) was the observed value less than the median of the null distribution

Supplementary Table 2: Number of features apparently engrafted, by number of patients that feature was engrafted in for each type of analysis.

Feature Type	Condition	# Patients	Feature Count
16S	Placebo	1	81
		2	35
		3	29
		4	11
		5	4
		6	3
		7	1
		8	0
		9	0
		10	1
	FMT (all)	1	109
		2	79
		3	40
		4	25
		5	10
		6	2
		7	0

		8	1
		9	0
		10	0
	FMT (responder)	1	118
		2	57
		3	33
		4	9
		5	3
		6	0
		7	1
	FMT (non-responder)	1	96
		2	33
		3	2
		4	0
		5	0
		6	0
		7	0
species	Placebo	1	80
		2	14
		3	3
		4	0
		5	0
	FMT (all)	1	158
		2	63
		3	24
		4	2
		5	5
	FMT (responder)	1	146
		2	49
		3	5
	FMT (non-responder)	1	90
		2	14
		3	4
strain	Placebo	1	13,080
		2	3,338
		3	750
		4	148
		5	20
		6	1
		7	0
		8	0

	FMT (all)	1	23,093
		2	10,316
		3	4,008
		4	1,229
		5	433
		6	129
		7	29
		8	1
	FMT (responder)	1	21,322
		2	7,281
		3	1,438
		4	162
	FMT (non-responder)	1	14,737
		2	3,084
		3	620
		4	51
MAG	Placebo	1	14
		2	2
		3	0
		4	0
		5	0
	FMT (all)	1	45
		2	17
		3	3
		4	0
		5	1
	FMT (responder)	1	39
		2	15
		3	1
	FMT (non-responder)	1	18
		2	0
		3	1
gene	Placebo	1	83,282
		2	11,775
		3	1,472
		4	142
		5	9
		6	0
		7	0
		8	0
	FMT (all)	1	218,257

		2	67,350
		3	18,043
		4	5,511
		5	713
		6	91
		7	11
		8	1
	FMT (responder)	1	176,849
		2	47,623
		3	3,766
		4	258
		5	5
	FMT (non-responder)	1	110,286
		2	16,322
		3	1,873
		4	78
		5	3

789
790
791 **Supplementary Table 3: The number of features apparently engrafted uniquely in FMT or**
792 **Placebo groups, or in both, by the total number of patients they appeared to be engrafted in**

Feature Type	Group Engrafted	Total Patients	Count
16S	FMT Only	1	73
		2	42
		3	18
		4	9
		5	4
	Placebo Only	1	31
		2	8
		3	4
		4	2
	Both	2	18
		3	20
		4	28
		5	19
		6	18
		7	5
		8	5
		9	3
		10	2
		12	1

		15	1
species	FMT Only	1	123
		2	48
		3	16
	Placebo Only	1	25
		2	6
		3	1
	Both	2	28
		3	20
		4	8
		5	4
		6	4
		7	1
strain	FMT Only	1	16,872
		2	6,594
		3	2,343
		4	552
		5	138
		6	67
		7	20
		8	1
	Placebo Only	1	3,589
		2	865
		3	193
		4	33
		5	6
	Both	2	4,618
		3	4,053
		4	2,245
		5	1,078
		6	474
		7	154
		8	26
		9	3
MAG	FMT Only	1	39
		2	16
		3	3
	Placebo Only	1	7
		2	1
	Both	2	5
		3	2

		6	1
gene	FMT Only	1	188,238
		2	50,809
		3	13,761
		4	4,654
		5	519
		6	61
		7	6
	Placebo Only	1	39,487
		2	4,672
		3	555
		4	35
		5	2
	Both	2	26,103
		3	16,986
		4	6,366
		5	1,858
		6	485
		7	95
		8	34
		9	2

795 ## References:

796

797 1. Kappelman, M. D. *et al.* The prevalence and geographic distribution of Crohn's disease and
798 ulcerative colitis in the United States. *Clin. Gastroenterol. Hepatol. Off. Clin. Pract. J. Am.*
799 *Gastroenterol. Assoc.* **5**, 1424–1429 (2007).
800 2. de Souza, H. S. P. & Fiocchi, C. Immunopathogenesis of IBD: current state of the art. *Nat. Rev.*
801 *Gastroenterol. Hepatol.* **13**, 13–27 (2016).
802 3. Hindryckx, P., Jairath, V. & D'Haens, G. Acute severe ulcerative colitis: from pathophysiology
803 to clinical management. *Nat. Rev. Gastroenterol. Hepatol.* **13**, 654–664 (2016).
804 4. Talley, N. J. *et al.* An evidence-based systematic review on medical therapies for
805 inflammatory bowel disease. *Am. J. Gastroenterol.* **106 Suppl 1**, S2-25; quiz S26 (2011).
806 5. Moayyedi, P. *et al.* Fecal Microbiota Transplantation Induces Remission in Patients With
807 Active Ulcerative Colitis in a Randomized Controlled Trial. *Gastroenterology* **149**, 102-109.e6
808 (2015).
809 6. Peery, A. F. *et al.* AGA Clinical Practice Guideline on Fecal Microbiota-Based Therapies for
810 Select Gastrointestinal Diseases. *Gastroenterology* **166**, 409–434 (2024).
811 7. Khoruts, A., Staley, C. & Sadowsky, M. J. Faecal microbiota transplantation for Clostridioides
812 difficile: mechanisms and pharmacology. *Nat. Rev. Gastroenterol. Hepatol.* **18**, 67–80 (2021).
813 8. Khanna, S., Shin, A. & Kelly, C. P. Management of Clostridium difficile Infection in
814 Inflammatory Bowel Disease: Expert Review from the Clinical Practice Updates Committee of
815 the AGA Institute. *Clin. Gastroenterol. Hepatol. Off. Clin. Pract. J. Am. Gastroenterol. Assoc.*
816 **15**, 166–174 (2017).

817 9. Feng, J. *et al.* Efficacy and safety of fecal microbiota transplantation in the treatment of
818 ulcerative colitis: a systematic review and meta-analysis. *Sci. Rep.* **13**, 14494 (2023).
819 10. Pai, N. *et al.* Results of the First Pilot Randomized Controlled Trial of Fecal Microbiota
820 Transplant In Pediatric Ulcerative Colitis: Lessons, Limitations, and Future Prospects.
821 *Gastroenterology* **161**, 388-393.e3 (2021).
822 11. Narula, N. *et al.* Systematic Review and Meta-analysis: Fecal Microbiota Transplantation
823 for Treatment of Active Ulcerative Colitis. *Inflamm. Bowel Dis.* **23**, 1702–1709 (2017).
824 12. Jaramillo, A. P. *et al.* Effectiveness of Fecal Microbiota Transplantation Treatment in
825 Patients With Recurrent Clostridium difficile Infection, Ulcerative Colitis, and Crohn's
826 Disease: A Systematic Review. *Cureus* **15**, e42120 (2023).
827 13. Liu, H., Li, J., Yuan, J., Huang, J. & Xu, Y. Fecal microbiota transplantation as a therapy for
828 treating ulcerative colitis: an overview of systematic reviews. *BMC Microbiol.* **23**, 371 (2023).
829 14. Smillie, C. S. *et al.* Strain Tracking Reveals the Determinants of Bacterial Engraftment in
830 the Human Gut Following Fecal Microbiota Transplantation. *Cell Host Microbe* **23**, 229-
831 240.e5 (2018).
832 15. Staley, C. *et al.* Durable Long-Term Bacterial Engraftment following Encapsulated Fecal
833 Microbiota Transplantation To Treat Clostridium difficile Infection. *mBio* **10**,
834 10.1128/mbio.01586-19 (2019).
835 16. Aggarwala, V. *et al.* Precise quantification of bacterial strains after fecal microbiota
836 transplantation delineates long-term engraftment and explains outcomes. *Nat. Microbiol.* **6**,
837 1309–1318 (2021).

838 17. Deng, Z.-L. *et al.* Engraftment of essential functions through multiple fecal microbiota
839 transplants in chronic antibiotic-resistant pouchitis—a case study using metatranscriptomics.
840 *Microbiome* **11**, 269 (2023).
841 18. Wilson, B. C. *et al.* Strain engraftment competition and functional augmentation in a
842 multi-donor fecal microbiota transplantation trial for obesity. *Microbiome* **9**, 107 (2021).
843 19. Podlesny, D. *et al.* Identification of clinical and ecological determinants of strain
844 engraftment after fecal microbiota transplantation using metagenomics. *Cell Rep. Med.* **3**,
845 100711 (2022).
846 20. Ianiro, G. *et al.* Variability of strain engraftment and predictability of microbiome
847 composition after fecal microbiota transplantation across different diseases. *Nat. Med.* **28**,
848 1913–1923 (2022).
849 21. Schmidt, T. S. B. *et al.* Drivers and determinants of strain dynamics following fecal
850 microbiota transplantation. *Nat. Med.* **28**, 1902–1912 (2022).
851 22. Lau, J. T. *et al.* Capturing the diversity of the human gut microbiota through culture-
852 enriched molecular profiling. *Genome Med.* **8**, 72 (2016).
853 23. Browne, H. P. *et al.* Culturing of 'unculturable' human microbiota reveals novel taxa and
854 extensive sporulation. *Nature* **533**, 543–546 (2016).
855 24. Sibley, C. D. *et al.* Culture Enriched Molecular Profiling of the Cystic Fibrosis Airway
856 Microbiome. *PLOS ONE* **6**, e22702 (2011).
857 25. Whelan, F. J. *et al.* Culture-enriched metagenomic sequencing enables in-depth profiling
858 of the cystic fibrosis lung microbiota. *Nat. Microbiol.* **5**, 379–390 (2020).

859 26. Myles, I. A. *et al.* A method for culturing Gram-negative skin microbiota. *BMC Microbiol.*
860 **16**, 60 (2016).
861 27. Hilt, E. E. *et al.* Urine Is Not Sterile: Use of Enhanced Urine Culture Techniques To Detect
862 Resident Bacterial Flora in the Adult Female Bladder. *J. Clin. Microbiol.* **52**, 871–876 (2014).
863 28. Callahan, B. J. *et al.* DADA2: High-resolution sample inference from Illumina amplicon
864 data. *Nat. Methods* **13**, 581–583 (2016).
865 29. Blanco-Míguez, A. *et al.* Extending and improving metagenomic taxonomic profiling with
866 uncharacterized species using MetaPhlAn 4. *Nat. Biotechnol.* **41**, 1633–1644 (2023).
867 30. Karcher, N. *et al.* Genomic diversity and ecology of human-associated Akkermansia
868 species in the gut microbiome revealed by extensive metagenomic assembly. *Genome Biol.*
869 **22**, 209 (2021).
870 31. Rousset, F. *et al.* Publisher Correction: The impact of genetic diversity on gene
871 essentiality within the Escherichia coli species. *Nat. Microbiol.* **6**, 700–700 (2021).
872 32. Meziti, A. *et al.* The Reliability of Metagenome-Assembled Genomes (MAGs) in
873 Representing Natural Populations: Insights from Comparing MAGs against Isolate Genomes
874 Derived from the Same Fecal Sample. *Appl. Environ. Microbiol.* **87**, e02593-20 (2021).
875 33. Franzosa, E. A. *et al.* Gut microbiome structure and metabolic activity in inflammatory
876 bowel disease. *Nat. Microbiol.* **4**, 293–305 (2019).
877 34. Montrose, J. A., Kurada, S. & Fischer, M. Current and future microbiome-based
878 therapies in inflammatory bowel disease. *Curr. Opin. Gastroenterol.*
879 10.1097/MOG.0000000000001027 doi:10.1097/MOG.0000000000001027.

880 35. Costello, S. P. *et al.* Effect of Fecal Microbiota Transplantation on 8-Week Remission in
881 Patients With Ulcerative Colitis: A Randomized Clinical Trial. *JAMA* **321**, 156–164 (2019).
882 36. Sieber, C. M. K. *et al.* Recovery of genomes from metagenomes via a dereplication,
883 aggregation and scoring strategy. *Nat. Microbiol.* **3**, 836–843 (2018).
884 37. Sczyrba, A. *et al.* Critical Assessment of Metagenome Interpretation-a benchmark of
885 metagenomics software. *Nat. Methods* **14**, 1063–1071 (2017).
886 38. Lewis, W. H., Tahon, G., Geesink, P., Sousa, D. Z. & Ettema, T. J. G. Innovations to
887 culturing the uncultured microbial majority. *Nat. Rev. Microbiol.* **19**, 225–240 (2021).
888 39. Forster, S. C. *et al.* A human gut bacterial genome and culture collection for improved
889 metagenomic analyses. *Nat. Biotechnol.* **37**, 186–192 (2019).
890 40. Whelan, F. J. *et al.* The loss of topography in the microbial communities of the upper
891 respiratory tract in the elderly. *Ann. Am. Thorac. Soc.* **11**, 513–521 (2014).
892 41. Bartram, A. K., Lynch, M. D. J., Stearns, J. C., Moreno-Hagelsieb, G. & Neufeld, J. D.
893 Generation of multimillion-sequence 16S rRNA gene libraries from complex microbial
894 communities by assembling paired-end illumina reads. *Appl. Environ. Microbiol.* **77**, 3846–
895 3852 (2011).
896 42. Martin, M. Cutadapt removes adapter sequences from high-throughput sequencing
897 reads. *EMBnet.journal* **17**, 10–12 (2011).
898 43. Quast, C. *et al.* The SILVA ribosomal RNA gene database project: improved data
899 processing and web-based tools. *Nucleic Acids Res.* **41**, D590–D596 (2013).
900 44. McMurdie, P. J. & Holmes, S. phyloseq: An R Package for Reproducible Interactive
901 Analysis and Graphics of Microbiome Census Data. *PLOS ONE* **8**, e61217 (2013).

902 45. Bolger, A. M., Lohse, M. & Usadel, B. Trimmomatic: a flexible trimmer for Illumina
903 sequence data. *Bioinformatics* **30**, 2114–2120 (2014).
904 46. Schmieder, R. & Edwards, R. Fast Identification and Removal of Sequence
905 Contamination from Genomic and Metagenomic Datasets. *PLOS ONE* **6**, e17288 (2011).
906 47. Nurk, S., Meleshko, D., Korobeynikov, A. & Pevzner, P. A. metaSPAdes: a new versatile
907 metagenomic assembler. *Genome Res.* **27**, 824–834 (2017).
908 48. Li, H. & Durbin, R. Fast and accurate short read alignment with Burrows–Wheeler
909 transform. *Bioinformatics* **25**, 1754–1760 (2009).
910 49. Kang, D. D. *et al.* MetaBAT 2: an adaptive binning algorithm for robust and efficient
911 genome reconstruction from metagenome assemblies. *PeerJ* **7**, e7359 (2019).
912 50. Parks, D. H., Imelfort, M., Skennerton, C. T., Hugenholtz, P. & Tyson, G. W. CheckM:
913 assessing the quality of microbial genomes recovered from isolates, single cells, and
914 metagenomes. *Genome Res.* **25**, 1043–1055 (2015).
915 51. Eren, A. M. *et al.* Community-led, integrated, reproducible multi-omics with anvi'o. *Nat.*
916 *Microbiol.* **6**, 3–6 (2021).
917 52. Chaumeil, P.-A., Mussig, A. J., Hugenholtz, P. & Parks, D. H. GTDB-Tk: a toolkit to classify
918 genomes with the Genome Taxonomy Database. *Bioinformatics* **36**, 1925–1927 (2020).
919 53. Price, M. N., Dehal, P. S. & Arkin, A. P. FastTree 2 – Approximately Maximum-Likelihood
920 Trees for Large Alignments. *PLOS ONE* **5**, e9490 (2010).
921 54. Schwengers, O. *et al.* Bakta: rapid and standardized annotation of bacterial genomes via
922 alignment-free sequence identification. *Microb. Genomics* **7**, 000685 (2021).

923 55. Shen, W., Le, S., Li, Y. & Hu, F. SeqKit: A Cross-Platform and Ultrafast Toolkit for FASTA/Q
924 File Manipulation. *PLOS ONE* **11**, e0163962 (2016).
925 56. Li, H. *et al.* The Sequence Alignment/Map format and SAMtools. *Bioinformatics* **25**,
926 2078–2079 (2009).
927 57. Camacho, C. *et al.* BLAST+: architecture and applications. *BMC Bioinformatics* **10**, 421
928 (2009).
929 58. Steinegger, M. & Söding, J. MMseqs2 enables sensitive protein sequence searching for
930 the analysis of massive data sets. *Nat. Biotechnol.* **35**, 1026–1028 (2017).
931 59. Cantalapiedra, C. P., Hernández-Plaza, A., Letunic, I., Bork, P. & Huerta-Cepas, J.
932 eggNOG-mapper v2: Functional Annotation, Orthology Assignments, and Domain Prediction
933 at the Metagenomic Scale. *Mol. Biol. Evol.* **38**, 5825–5829 (2021).
934 60. Wickham, H. *et al.* Welcome to the Tidyverse. *J. Open Source Softw.* **4**, 1686 (2019).
935